Influence of Strain on Space Charge Distribution at Ferroelectric Thin-Film Free Surfaces (to appear in Acta Materialia)

Lun Yang* and Kaushik Dayal†
Carnegie Mellon University

August 1, 2012

Abstract

Ferroelectric perovskites are wide-bandgap semiconductors and therefore are often modeled as perfect dielectrics. However, space charges can play an important role in regions with large electric fields, such as at domain walls, free surfaces, near electrodes, and so on. In this paper, we apply a mesoscale model to examine the space charge distribution at free-surface closure domain patterns in a ferroelectric thin-film. The model uses a conventional electromechanical phase-field approach for ferroelectric domain patterns in combination with drift-diffusion based equations to model space-charge distribution. We additionally apply a boundary element method to compute the stray electric fields outside the ferroelectric free surface. We probe the influence of mechanical strain, such as would be applied through a substrate, on the distribution of space-charge. We find an indirect, but strong, coupling between mechanics and space-charge distribution. The physical mechanism of this coupling is as follows: the mechanical strain induces changes in the domain patterns and polarization distribution; this in turn changes the local electric fields sufficiently that space charges are redistributed on the free surface rather than moving towards the bottom electrode. We note two interesting features of this coupling: first, the coupling mechanism is operative only at free surfaces due to the complex domain patterns in these regions, and would not occur in the bulk; second, though domain patterns are visually only marginally changed by the presence of space-charges, the changes in electric field due to these seemingly small changes is significant and this provides the coupling with space-charge.

1 Introduction

Ferroelectric perovskites are widely used in devices that exploit their spontaneous polarization and the ability to switch this polarization, e.g. high-speed memories [Sco00] and sensors [Xu91, Uch96]. Modeling techniques, such as phase-field approaches, have followed these applications and therefore typically treated ferroelectrics as insulators [Che02, SB01, ZB05, DB07, YD11c, LYSL10, LLSL11]. How-

*lunyang@cmu.edu
†kaushik@cmu.edu

ever, in recent applications, particularly in thin-film geometries, the the semiconducting nature of ferroelectrics and the role of space charges has become important. For instance, the interactions between light, space-charges and ferroelectric domain structures are exploited for optoelectronics and photovoltaics [FGDN08, YSB$^+$10, SFY$^+$11]. In addition, space charge interactions with domain walls and leakage currents due to space charge motion in thin films can lead to reduced performance, e.g. [CHN$^+$02, XSB05]. Recent experiments have shown the possibility of surface domain patterns persisting above the Curie temperature, possibly due to space charges clustering at the electric field inhomogeneities at surface domain walls below Curie temperature [HFD$^+$12]. Therefore, there have been recent efforts to develop models of ferroelectrics that couple the microstructure evolution to the evolution of space charge and solve for both these together [XB08, ZLF10, SB12].

Space charges are typically important in regions with inhomogeneous electric fields. In addition to domain walls, inhomogeneous fields often arise due to geometric features, e.g. cracks, free surfaces, edges of electrodes. The challenge in these geometries is that electric fields are not confined to the ferroelectric but exist in the surrounding vacuum as well. Therefore, modeling methods must account for the fact that the electrostatic problem is posed on an infinite domain. Our focus in this paper is the interaction of space charges with the complex closure domain patterns at ferroelectric free surfaces, in particular taking into account that space-charges are both driven by domain patterns but also can drive evolution of the domain patterns. While this issue has been studied by various researchers, previous work has involved various approximations. For instance, we have examined the formation of closure domains at a free surface under various geometries and boundary conditions [YD11b, DB07] and space charges were specified and not free to evolve. These studies showed that large electric fields and complex domain patterns form at free surfaces, making it likely that space charges will play an important role. In [KB01], the role of space charges at free surfaces was examined in detail both experimentally and theoretically. The theoretical analysis assumed that domain patterns were fixed and did not evolve in response to space charges. A series of papers by Watanabe have examined this question in great detail both theoretically and experimentally [WOM01, Wat98, Wat10, WM01, Wat11]. A key conclusion from this work is that intrinsic charge carriers, i.e., not external charge compensation from the ambient, is required to explain certain experimental results conducted in UHV. However, to enable mathematical analysis, the theoretical models in these papers use very simplified domain patterns and do not model the more complex domain patterns.

In this paper, we apply a recent model that couples Ginzburg-Landau phase-field models to drift-diffusion based equations for space charge evolution [XB08, ZLF10, SB12, LL10]. To solve the equations of equilibrium, we use a numerical procedure that we have developed [YD11a]; the key feature of this procedure is that it provides an efficient iterative approach to evolve the polarization and the space charge while *consistently* transforming the infinite domain electrostatic problem to a finite domain with equivalent boundary conditions. This enables us to study the evolution of polarization and space charge at a ferroelectric thin-film free surface. In addition, we also examine the role of applied strain, e.g. induced by the film substrate, on the behavior of space charges. We find an indirect, but strong, coupling between mechanical strain and the space-charge distribution. The physical mechanism of this coupling is as follows: the mechanical strain induces changes in the domain patterns and polarization distribution; this in turn changes the local electric fields sufficiently that space charges are redistributed on the free surface rather than moving towards the bottom electrode. We note two interesting features of this coupling: first, the coupling mechanism is operative only at free surfaces due to the complex domain patterns in these regions, and would not occur in the bulk; second, though domain patterns are visually only marginally changed by the presence of space-charges, the changes in electric field due to these seemingly small changes is significant and this provides the coupling with space-charge.

This paper is organized as follows. In Section 2, we describe the model. In Section 3, we outline the solution technique. In Section 4, we describe the results of our calculations on space charge and domain patterns at free surfaces under different applied strains. We conclude in Section 5.

2 Phase-Field Model Coupled to Space Charge Drift-Diffusion Equations

The energy E of a ferroelectric specimen occupying a region Ω (Fig. 1(a)) is written as [SB01]:

$$E[\boldsymbol{\epsilon}, \boldsymbol{p}] = \int_{\Omega} \left[U(\nabla \boldsymbol{p}) + W(\boldsymbol{\epsilon}, \boldsymbol{p}, n_c, p_v, {N_d}^+, {N_d}^0) \right] \, d\Omega + \frac{\epsilon_0}{2} \int_{\mathbb{R}^3} |\nabla \phi|^2 \, dV \tag{2.1}$$

E is a functional of the strain field $\boldsymbol{\epsilon}(\boldsymbol{x})$, the polarization field $\boldsymbol{p}(\boldsymbol{x})$, and the concentrations of electrons in the conduction band n_c, holes p_v in the valence band, ionized donors N_d^+, and non-ionized donors N_d^0 [XB08, SB12]. Additional terms from applied electric fields and mechanical loads are added if these are present.

The term $U(\nabla \boldsymbol{p})$ models the contribution from domain walls and prevents them from becoming infinitely sharp; the contribution from W is assumed to be additively decomposed:

$$W(\boldsymbol{\epsilon}, \boldsymbol{p}, n_c, p_v, {N_d}^+, {N_d}^0) = W_1(\boldsymbol{\epsilon}, \boldsymbol{p}) + W_2(n_c) + W_3(p_v) + W_4({N_d}^+, {N_d}^0) \tag{2.2}$$

and finally, the last integral over all of space is the energy due to the electric potential ϕ. The electric field ϕ is coupled to the polarization and space charge distribution through the electrostatic equation:

$$\nabla \cdot (\boldsymbol{p} - \epsilon_0 \nabla \phi) = \rho \text{ over } \mathbb{R}^3, \quad \rho = q \left({N_d}^+ - n_c + p_v \right). \tag{2.3}$$

where q is the magnitude of the electronic charge. Therefore, though the additive decomposition of W into contributions from each species suggests that each species evolves independently, they are tightly coupled through the electrostatic interactions.

The specific forms of $W_2(n_c), W_3(p_v), W_4({N_d}^+, {N_d}^0)$ come from standard equilibrium statistical mechanics arguments. Taking the variation of E with respect to $n_c, p_v, {N_d}^+$, but with the constraint of conservation of species, gives us the evolution of space charges accounting for diffusion, drift and species interconversion. We note that these equations are very similar to, but slightly different from, the standard semiconductor drift-diffusion equations.

$$\begin{aligned}
\dot{n}_c &= \nabla \cdot (K_1 \nabla \mu_{n_c}) + k_1 N_d^0 (1 - e^{\beta(\mu_{n_c} + \mu_{{N_d}^+} - \mu_{{N_d}^0})}) + k_2 P (1 - e^{\beta(\mu_{n_c} + \mu_{p_v})}) \text{ on } \Omega, \\
\dot{p}_v &= \nabla \cdot (K_2 \nabla \mu_{p_v}) + k_2 P (1 - e^{\beta(\mu_{n_c} + \mu_{p_v})}) + k_3 {N_d}^+ (1 - e^{\beta(\mu_{p_v} + \mu_{{N_d}^0} - \mu_{{N_d}^+})}) \text{ on } \Omega, \\
\dot{N}_d^+ &= k_1 N_d^0 (1 - e^{\beta(\mu_{n_c} + \mu_{{N_d}^+} - \mu_{{N_d}^0})}) - k_3 {N_d}^+ (1 - e^{\beta(\mu_{p_v} + \mu_{{N_d}^0} - \mu_{{N_d}^+})}) \text{ on } \Omega, \\
\dot{N}_d^0 &= -\dot{N}_d^+
\end{aligned} \tag{2.4}$$

Here, we have assumed that the donors do not diffuse but change their concentration only due to local interconversion between species.

The chemical potentials $\mu_{n_c}, \mu_{p_v}, \mu_{N_d^0} - \mu_{N_d^+}$ are

$$\mu_{n_c} = E_c - \frac{1}{\beta} \log\left(\frac{N - n_c}{n_c}\right) - q\phi, \mu_{p_v} = -E_v + \frac{1}{\beta} \log\left(\frac{p_v}{P - p_v}\right) + q\phi, \mu_{{N_d}^0} - \mu_{{N_d}^+} = E_d - \frac{1}{\beta} \log\left(\frac{2{N_d}^+}{{N_d}^0}\right) - q\phi \tag{2.5}$$

Here, $\beta = (kT)^{-1}$ and N, P are the density of states in the conduction and valence bands respectively. The energies of the valence, donor, and conduction bands are E_v, E_d, E_c respectively. k_1, k_2, k_3 are rate constants for the species interconversion reactions.

The boundary conditions for the space charge evolution are:

$$K_1 \nabla \mu_{n_c} \cdot \boldsymbol{n} = k_4 (e^{\beta(\mu_{n_c} + \Phi)} - 1) \text{ on } S_1, K_1 \nabla \mu_{n_c} \cdot \boldsymbol{n} = 0 \text{ on } S_2, K_2 \nabla \mu_{p_v} \cdot \boldsymbol{n} = 0 \text{ on } S \tag{2.6}$$

Here, Φ is the work function of the bottom electrode S_1, and $\boldsymbol{n}$ is the outward normal of the boundary $S = S_1 \cup S_2$ of Ω.

We refer the reader [XB08, SB12] for the full details of the derivation of the space charge evolution model as well as the specific numerical parameters for barium titanate that we model here.

As we evolve the above equations, we must also minimize E over all admissible strain and polarization fields and satisfy the electrostatic equation. The first variation of E with respect to $\boldsymbol{p}$ gives the following gradient flow equation [YD11c]:

$$\dot{\boldsymbol{p}} \sim \nabla \cdot \left(\frac{\partial U}{\partial \nabla \boldsymbol{p}} \right) - \frac{\partial W_1}{\partial \boldsymbol{p}} - \nabla \phi \text{ on } \Omega, \boldsymbol{n} \cdot \left(\frac{\partial U}{\partial \nabla \boldsymbol{p}} \right) = 0 \text{ on } S \tag{2.7}$$

At each iteration of this evolution, we assume that mechanical equilibrium holds and solve $\nabla \cdot \left(\frac{\partial W}{\partial \nabla \boldsymbol{\epsilon}} \right) = 0$ with the mechanical boundary conditions described below.

We use barium titanate in two dimensions as our model material. The full details of the Ginzburg Landau polynomial chosen for W_1 to models barium titanate is given in [YD12]. The length units on all figures correspond to nanometers. In the nondimensionalized units for voltage, the breakdown field is $O(50)$.

3 The Problem Setup and Solution Method

Our solution strategy to find equilibrium domain patterns and space charge distributions is as follows. At each time step, we update the polarization and the space charge concentration fields. For the electrostatic equation that is posed on all of space, we apply an iterative inverse method [YD11a] that replaces the all-space problem by a finite domain problem with consistently transformed boundary conditions. We link the iterations of this method to the time-stepping that is used to update the polarization and space charge fields. At each step of this process, we also solve mechanical equilibrium to obtain the updated strain fields.

The spatial discretization of $\boldsymbol{p}$, ϕ, n_c, p_v, ${N_d}^+$ use standard finite element methods (FEM) with triangle elements and linear shape functions. The mechanical equilibrium equation is solved with the same approach but using the displacement field $\boldsymbol{u}(\boldsymbol{x})$ as the primary variable. Time-stepping uses a linearly implicit method [YD11c] until the system reaches equilibrium. We ensure that we have reached equilibrium by examining when the right side of (2.4) and (2.7) are small. We use synchronous time-stepping, i.e., all equations are evolved at the timescale set by the fastest process. We note that since this is an equilibrium calculation, only the relative values of the diffusion and rate constants K_1, K_2, k_1, k_2 and k_3 are of relevance, as noted also in [SB12].

Fig. 1(a) shows the computational domain with the mesh and the boundary conditions. For the mechanics, we apply displacement boundary conditions on the bottom and both sides, and the top surface is

traction-free. On the sides, we use the displacement boundary condition $u_2 = \epsilon^0_{22} x_2$, where ϵ^0_{22} is the 22 component of the stress-free strain. At the bottom, we model the substrate-induced strain by using the displacement boundary condition $u_1 = \alpha \epsilon^0_{11} x_1$. When $\alpha = 1.0$, this provides a stress-free setting; when $\alpha < 1.0$, this implies a horizontal extension because $\epsilon^0_{11} < 0$.

The electrical boundary conditions are that the bottom of the film is electroded and set to ground ($\phi = 0$). We chose the electrodes at the bottom with work function $\Phi = 4.3$ to model silver. From previous work [DB07, YD11b], it is known that closure domain patterns at the surface create large fields.

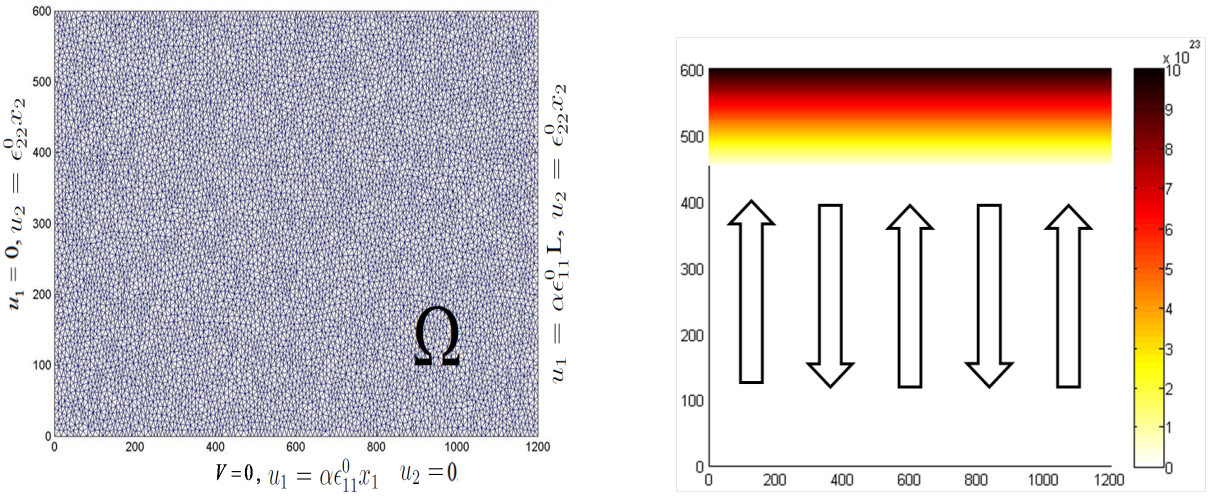

(a) (b)

Figure 1: (a) Finite Element mesh and boundary conditions. $\boldsymbol{\epsilon}^0$ is the stress-free strain, and α is a parameter to denote the level of applied strain. The bottom of the film is connected to a grounded electrode with work function $\Phi = 4.3$ to model silver. (b) The initial guess for the domain patterns is a series of simple 180 domains, and the initial guess for the non-ionized donor concentration N^0_d is a linear profile that reaches zero some depth from the surface. At the initial state, we also assume that there are no ionized donors, electrons, or holes; these are created due to the electric field as the calculation evolves.

4 Space Charge Distribution at a Free Surface with Closure Domains

In this section, we apply the model to study the interactions between domain patterns and space charge at free-surface closure domains. We focus on equilibrium distributions of space charge and domain patterns, but apply different strain boundary conditions to model the effect of strain tuning through the substrate. The thin-film is grounded through the bottom electrode.

We begin by studying the case of a thin-film on a substrate that is perfectly matched to the stress-free spontaneous state of the ferroelectric when it has the 180° domain pattern shown in Fig. 1(b). To achieve this, we set $\alpha = 1.0$ using the notation in Fig. 1(a). Figures 2(a), 3(a), and 4(a) show the equilibrium distributions of the polarization, electric potential and space charge density respectively. We note certain features of the solution. First, the polarization distribution and domain patterns are visually very similar to the closure domain patterns observed in ferroelectric phase-field calculations that do not include space charges [YD11b, DB07]. The electric potential looks qualitatively similar to the case without space

charges, and the 90° domain walls are clearly visible. However, in comparison to the case without space charge, the potential field is slightly more diffuse implying that the electric fields are smaller due to the effect of space charges. The space charge distribution, Fig. 4(a), shows that the primary motion of electrons is away from the electric fields at the free surface towards the grounded bottom electrode leaving a layer of positive charges (holes) at the surface. The maximum magnitude of the positive charge concentration is fairly close to that of the donor concentration because a large fraction of the donors are ionized and many of the free electrons have moved towards the grounded bottom electrode. The arrows in Fig. 4 indicate the movements of electrons.

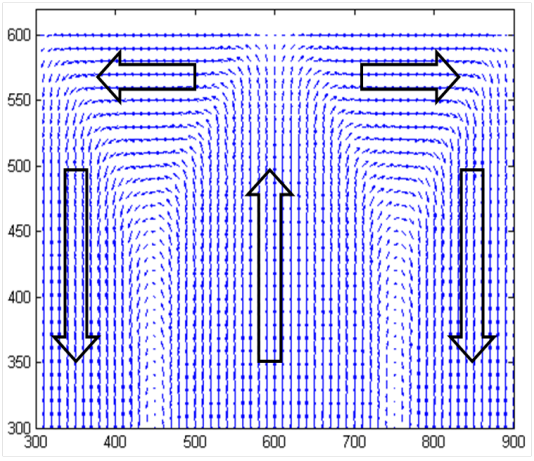

(a) $\alpha = 1.0$.

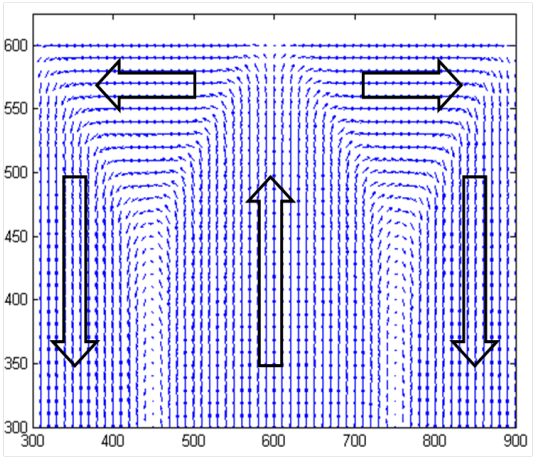

(b) $\alpha = 0.5$.

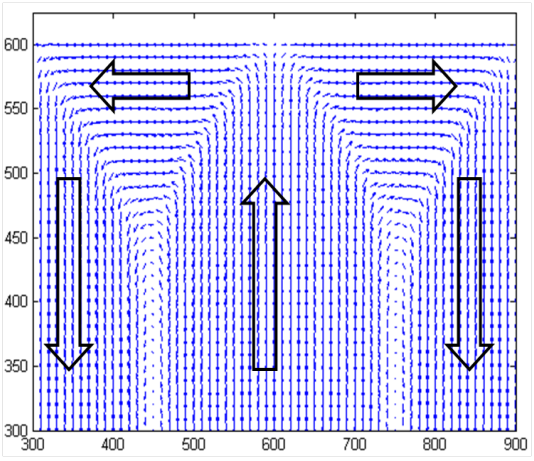

(c) $\alpha = 0$.

Figure 2: Closure domain patterns under different mechanical boundary conditions: (1) $\alpha = 1.0$ represents the spontaneous strain, (2) $\alpha = 0.5$, (3) $\alpha = 0$. Visually, these are almost identical. Very small differences at domain walls lead to different electric potential fields.

We now apply a moderate tensile strain through the substrate by setting α to 0.5. We use the same initial conditions as previously and evolve the system until it reaches equilibrium. Figs. 2(b), 3(b) and 4(b) show the equilibrium distributions of the polarization, electric potential and space charge density respectively. Previous studies [YD11b] without space charges show that the electromechanical coupling in ferroelectrics in combination with the complex closure domain patterns causes an increase in electric potential and field when the specimen is subject to stress. This is qualitatively in agreement with our finding here in Fig. 3(b). While the magnitude of the potential increases only marginally, the region of

high potential becomes larger and more diffuse. This is driven both by electromechanics of the domain pattern as well as the redistribution of space charges. This is driven primarily by the following physical mechanism: the mechanical strain causes domain patterns to reorient and change slightly when compared visually, but this is sufficient to cause a moderate change in voltage due to the change in bound charges at the domain walls. This moderate change in voltage translates to a large change in space-charge distribution, Fig. 4(b). We observe that free electrons move not just towards the electrodes but also rearrange themselves on the free surface, in particular attracted towards the larger region of high potential directly above the upward-pointing domain. As the figure shows, the free surface consequently becomes negatively charged in that region. A somewhat analogous result is reported in [XSB05] where negative charges are observed at 90° domain wall where the potential is sufficiently large.

Finally, we apply a much larger tensile strain using $\alpha = 0$, corresponding to a strain that sets the c dimension of the tetragonal unit cell size to the value of the cubic paraelectric phase. Figs. 2(c), 3(c) and 4(c) show the equilibrium distributions of the polarization, electric potential and space charge density respectively. Qualitatively our conclusions are similar to the case when $\alpha = 0.5$ but more pronounced. The domain patterns are visually almost unchanged while the potential is slightly more diffuse. The space charge region has a negative region with significant extent at the free surface, growing at the expense of the neutral region while the positive region is not significantly changed from the strain-free case ($\alpha = 1.0$).

5 Discussion

In this paper, we have simulated the combined evolution of domain patterns and space charge distribution at a ferroelectric free surface using a combined phase-field model (for domain patterns) and a drift-diffusion based model (for space charge). In addition, we also examine the role of applied strain, e.g. induced by the film substrate, on the behavior of space charges. Our key finding is an indirect, but significant, coupling between mechanical strain and the space-charge distribution. In particular, when the substrate strain matches the spontaneous strain of the ferroelectric, the free electrons mostly move towards the bottom electrode that is grounded. However, as a tensile strain is applied, the free-surface closure domain patterns change very slightly, but sufficiently that they induce changes in the electric potential field. This then causes a significant number of the free electrons to redistribute themselves on the free surface leading to the formation of a negatively charged region on the surface. Our finding is robust in that these conclusions are unchanged even when the substrate strain is enhanced significantly.

We note two interesting features of this strong mechanical-to-space-charge coupling. First, this coupling requires the presence of 90° domain walls due to closure domains to be operative. In a bulk specimen consisting of antiparallel domains alone, mechanical stresses alone cannot cause significant space-charge redistribution. Consequently, this mechanism is a feature of thin-films and free surfaces, or requires other complex microstructural features to enable this coupling. Second, though domain patterns are visually only marginally changed by the presence of space-charges, the changes in electric field due to these seemingly small changes is significant and this provides the coupling with space-charge.

We close by mentioning possible applications and experimental tests. First, recent experiments have shown the possibility of using non-180° domain walls and domain patterns for photovoltaic applications with the possibility of significant open-circuit voltages [YSB$^+$10, SFY$^+$11]. Mechanical strain induced through the substrate provides a practical mechanism to potentially enhance the voltage. Second, [Wat11]

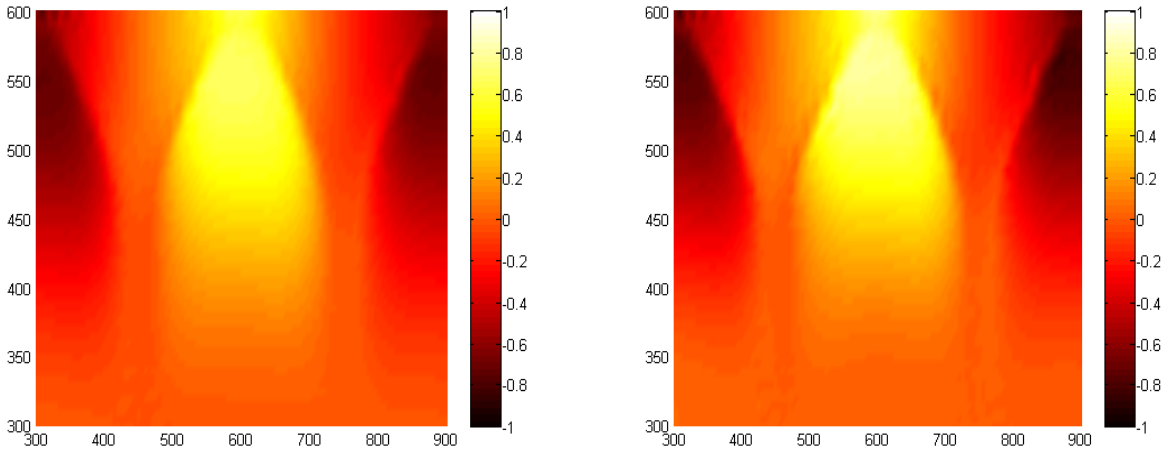

(a) $\alpha = 1.0$.

(b) $\alpha = 0.5$.

(c) $\alpha = 0$.

Figure 3: Closure domain electric potential field with different mechanical boundary conditions.

recently reported careful measurements of the ferroelectric free surface in UHV, thus removing the influence of external charge compensation. Also, [JS09] measured surface charges on a ferroelectric sample in ambient conditions. Similar experiments, if carried out with applied strain, can elucidate the mechanism of space charge distribution on the ferroelectric free surface.

Acknowledgment

This research was supported in part by the National Science Foundation through TeraGrid resources provided by the Pittsburgh Supercomputing Center. The real-space phase-field program that we have developed to obtain the results described in this paper is available at www.matforge.org. Kaushik Dayal thanks ARO Numerical Analysis for financial support. Lun Yang thanks Carnegie Mellon University for financial support through the Liang Ji-Dian Fellowship.

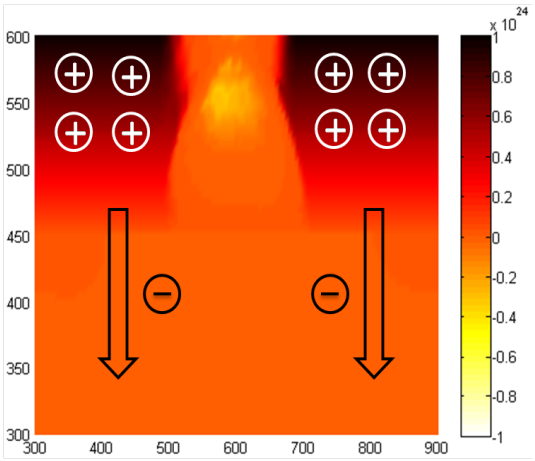

(a) $\alpha = 1.0$.

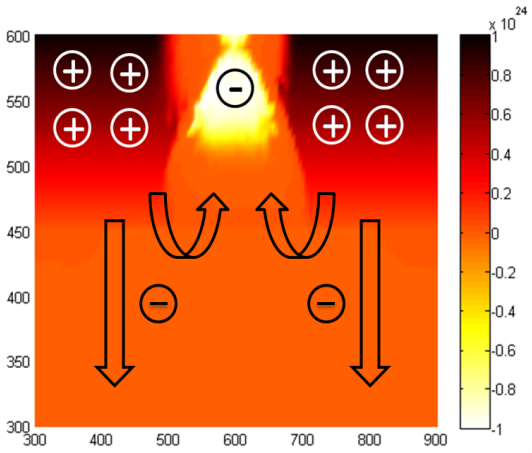

(b) $\alpha = 0.5$.

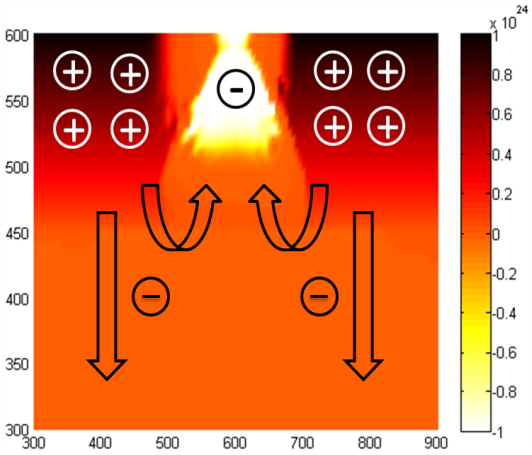

(c) $\alpha = 0$.

Figure 4: Space charge distribution with different mechanical boundary conditions. The black arrows indicate the movement of electrons.

References

[Che02] L.Q. Chen, *Phase-field models for microstructure evolution*, Annual review of materials research **32** (2002), no. 1, 113–140.

[CHN+02] MW Cole, C. Hubbard, E. Ngo, M. Ervin, M. Wood, and RG Geyer, *Structure–property relationships in pure and acceptor-doped basrtio thin films for tunable microwave device applications*, Journal of applied physics **92** (2002), 475.

[DB07] K. Dayal and K. Bhattacharya, *A real-space non-local phase-field model of ferroelectric domain patterns in complex geometries*, Acta materialia **55** (2007), no. 6, 1907–1917.

[FGDN08] P. Ferraro, S. Grilli, and P. De Natale, *Ferroelectric crystals for photonic applications: including nanoscale fabrication and characterization techniques*, vol. 91, Springer Verlag, 2008.

[HFD+12] A. Höfer, M. Fechner, K. Duncker, M. Hölzer, I. Mertig, and W. Widdra, *Persistence of surface domain structures for a bulk ferroelectric above t_ {C}*, Physical Review Letters **108** (2012), no. 8, 087602.

[JS09] F. Johann and E. Soergel, *Quantitative measurement of the surface charge density*, Applied Physics Letters **95** (2009), 232906.

[KB01] S.V. Kalinin and D.A. Bonnell, *Local potential and polarization screening on ferroelectric surfaces*, Physical Review B **63** (2001), no. 12, 125411.

[LL10] YY Liu and JY Li, *Space charges and size effects in semiconducting ferroelectric batio/srtio superlattices*, Applied Physics Letters **97** (2010), 042905.

[LLSL11] LJ Li, CH Lei, YC Shu, and JY Li, *Phase-field simulation of magnetoelastic couplings in ferromagnetic shape memory alloys*, Acta Materialia (2011).

[LYSL10] LJ Li, Y. Yang, YC Shu, and JY Li, *Continuum theory and phase-field simulation of magnetoelectric effects in multiferroic bismuth ferrite*, Journal of the Mechanics and Physics of Solids **58** (2010), no. 10, 1613–1627.

[SB01] YC Shu and K. Bhattacharya, *Domain patterns and macroscopic behaviour of ferroelectric materials*, Philosophical Magazine Part B **81** (2001), no. 12, 2021–2054.

[SB12] P. Suryanarayana and K. Bhattacharya, *Evolution of polarization and space charges in semiconducting ferroelectrics*, Journal of Applied Physics **111** (2012), 034109.

[Sco00] J.F. Scott, *Ferroelectric memories*, Springer Verlag, 2000.

[SFY+11] J. Seidel, D. Fu, S.Y. Yang, E. Alarcón-Lladó, J. Wu, R. Ramesh, and J.W. Ager III, *Efficient photovoltaic current generation at ferroelectric domain walls*, Physical Review Letters **107** (2011), no. 12, 126805.

[Uch96] K. Uchino, *Piezoelectric actuators and ultrasonic motors*, Kluwer, 1996.

[Wat98] Y. Watanabe, *Theoretical stability of the polarization in a thin semiconducting ferroelectric*, Physical Review B **57** (1998), no. 2, 789.

[Wat10] ———, *Apparent closure domain by standard 180 domain theory and necessity of fundamental screening in the theory*, Ferroelectrics **401** (2010), no. 1, 61–64.

[Wat11] ———, *Properties of clean surface of batio3 single crystals in uhv and virtual absence of nonferroelectric surface layer*, Ferroelectrics **419** (2011), no. 1, 28–32.

[WM01] Y. Watanabe and A. Masuda, *Theoretical stability of polarization in metal/ferroelectric/insulator/semiconductor and related structures*, Japanese Journal of Applied Physics **40** (2001), 5610.

[WOM01] Y. Watanabe, M. Okano, and A. Masuda, *Surface conduction on insulating batio_ {3} crystal suggesting an intrinsic surface electron layer*, Physical Review Letters **86** (2001), no. 2, 332–335.

[XB08] Y. Xiao and K. Bhattacharya, *A continuum theory of deformable, semiconducting ferroelectrics*, Archive for Rational Mechanics and Analysis **189** (2008), no. 1, 59–95.

[XSB05] Y. Xiao, V.B. Shenoy, and K. Bhattacharya, *Depletion layers and domain walls in semiconducting ferroelectric thin films*, Physical review letters **95** (2005), no. 24, 247603.

[Xu91] Y. Xu, *Ferroelectric materials and their applications*, North-Holland, 1991.

[YD11a] Lun Yang and Kaushik Dayal, *A completely iterative method for the infinite domain electrostatic problem with nonlinear dielectric media*, Journal of Computational Physics **230** (2011), no. 21, 7821 – 7829.

[YD11b] _____, *Effect of lattice orientation, surface modulation, and applied fields on free-surface domain microstructure in ferroelectrics*, Acta Materialia **59** (2011), no. 17, 6594 – 6603.

[YD11c] _____, *Microstructure and stray electric fields at surface cracks in ferroelectrics*, To appear in Intl. J. Fracture (2011).

[YD12] L. Yang and K. Dayal, *Free surface domain nucleation in a ferroelectric under an electrically charged tip*, Journal of Applied Physics **111** (2012), no. 1, 014106–014106.

[YSB+10] SY Yang, J. Seidel, SJ Byrnes, P. Shafer, C.H. Yang, MD Rossell, P. Yu, Y.H. Chu, JF Scott, JW Ager, et al., *Above-bandgap voltages from ferroelectric photovoltaic devices*, Nature Nanotechnology **5** (2010), no. 2, 143–147.

[ZB05] W. Zhang and K. Bhattacharya, *A computational model of ferroelectric domains. Part I: model formulation and domain switching*, Acta materialia **53** (2005), no. 1, 185–198.

[ZLF10] Y. Zhang, J. Li, and D. Fang, *Oxygen-vacancy-induced memory effect and large recoverable strain in a barium titanate single crystal*, Physical Review B **82** (2010), no. 6, 064103.